J Solid State Electrochem (2002) 6: 231 – 236
DOI 10.1007/s100080100226

ORIGINAL PAPER

R. Valaski · S. Ayoub · L. Micaroni · I.A. Hümmelgen

Polypyrrole-poly(3-methylthiophene) bilayer films electrochemically deposited onto tin oxide

Received: 26 April 2001 / Accepted: 15 May 2001 / Published online: 20 July 2001

Abstract We report the electrochemical successive deposition of layers of polypyrrole and poly(3-methylthiophene), forming conjugated polymer heterostructures onto a tin oxide-covered glass substrate. The polymer bilayer thickness and roughness were determined as a function of deposition conditions, varying the sequence of deposition of the conjugated polymer layers. The charge transport characteristics of these bilayer devices were investigated and an effective charge carrier mobility of the order of 10^{-10} cm^2 V^{-1} s^{-1} was determined.

Keywords Electrical properties and measurements · Organic semiconductors · Polymers · Tin oxide · Electrochemical bilayer deposition

Introduction

In recent years, several organic electronic and optoelectronic devices based on doped and undoped semiconducting polymers have been demonstrated. In some cases, like light-emitting diodes and photovoltaic devices, better performances were achieved in multilayered structures. These structures may permit or improve exciton dissociation or introduce additional potential barriers that confine or impose limits to charge carrier transport, benefiting device efficiency [1, 2, 3, 4, 5, 6].

The preparation of polymeric multilayered structures, however, may be difficult in practice. The deposition of a layer using the most common adopted procedure, spin coating, may partially or completely dissolve previously prepared layers. As a consequence, desired material combinations, interesting from the point of view of the physical characteristics of the polymers, are not always simple to produce owing to limitations imposed by solvent compatibility.

Electrochemical preparations of heterojunctions consisting of conjugated polymer bilayers have been reported and the corresponding bilayer devices have demonstrated rectifying characteristics [7, 8, 9, 10].

In this paper we address this problem of conjugated polymer multilayer deposition, presenting results on the electrochemical deposition and characterization of bilayer thin films of PPy/PMeT and PMeT/PPy [PPy: polypyrrole; PMeT: poly(3-methylthiophene)] onto a tin oxide (TO) substrate. Monolayer electrochemical deposition of PPy and PMeT onto TO was the subject of recent reports [11, 12].

Experimental

PMeT and PPy films were prepared using TO-covered glass plates as substrate. TO films were prepared on glass substrates using reactive chemical vapor deposition [13]. The TO films were formed through the reaction $SnCl_2 + O_2 \rightarrow SnO_2 + Cl_2$ (onto glass substrate at 550 °C in air). Deposition conditions were adjusted in order to produce TO films with a thickness of 193 ± 20 nm, arithmetic average roughness [14] R_a of 2.5 ± 0.7 nm and electrical resistivity ρ of 3.1×10^{-3} Ω cm. The TO films produced under these conditions present a work function of $\phi_{TO} \approx 4.3$ eV [15].

PPy films were galvanostatically deposited onto TO or TO/PMeT in a single-compartment cell with two electrodes (the applied current density j_d was constant and equal to 1.0 mA cm^{-2}) [12]. The electrolyte was a 0.05 mol L^{-1} solution of tetramethylammonium tetrafluoroborate (Me_4NBF_4) in acetonitrile containing pyrrole monomer in 0.1 mol L^{-1} concentration.

PMeT films were galvanostatically deposited onto TO or TO/PPy, also in a single-compartment cell with two electrodes (the applied current density j_d was constant and equal to 3.75 mA cm^{-2}) [11]. The synthesis electrolyte was a 0.02 mol L^{-1} Me_4NBF_4 solution in acetonitrile containing MeT monomer in 0.1 mol L^{-1} concentration.

The deposited film area was around 7×5 mm^2. Film thickness and roughness were determined using a surface profiler. On double polymer layer samples the thickness of the second layer was determined by subtracting the first layer measured thickness from the double layer measured thickness. Micrographs of the polymers

R. Valaski · I.A. Hümmelgen (✉)
Departamento de Física, Universidade Federal do Paraná, Caixa Postal 19044, 81531-990 Curitiba PR, Brazil
E-mail: iah@fisica.ufpr.br

S. Ayoub · L. Micaroni
Departamento de Química, Universidade Federal do Paraná, Caixa Postal 19081, 81531-990 Curitiba PR, Brazil

films were made in a scanning electron microscope (SEM), operating at 10 kV.

For the optical measurements we used the cell described above. The electrolyte was 0.1 mol L^{-1} Me_4NBF_4 solution in acetonitrile and the reference electrode was Ag/AgCl. The absorption spectra were measured by polarizing the films onto TO substrate to –0.5 V versus Ag/AgCl [12]. The samples for electrical measurements were prepared in a TO/PPy/PMeT/Al or TO/PMeT/PPy/Al sandwich structure. Al films ($\phi_{Al}\approx4.3$ eV [16]) were deposited onto glass by thermal evaporation. Contact geometry details have been published elsewhere [17].

The current versus voltage, $I(V)$, characteristics of the devices were determined by increasing the applied voltage stepwise (steps of 0.03 V) at a rate of 0.03 V s^{-1}.

Results and discussion

Layer thickness and morphology

In Table 1 we present the thickness of PMeT (d_{PMeT}) and PPy (d_{PPy}) films, in both cases homolayers, grown on TO as a function of charge density, Q:

$$Q\left(Q=\int_0^t j_d\,dt\right) \quad (1)$$

Table 1 PMeT and PPy film thickness as a function of charge density

Q (mC cm^{-2})	d_{PMeT} (nm)	d_{PPy} (nm)
100	207.4 ± 35.1	495.8 ± 80.7
75	152.9 ± 29.4	362.5 ± 23.2
50	132.5 ± 12.7	259.8 ± 18.4
35	113.8 ± 54.2	125.8 ± 27.5
25	100.2 ± 18.6	100.8 ± 12.4

where t is the deposition time, with j_d assuming the value specified above.

Table 2 presents the thickness of the PMeT layer of TO/PPy/PMeT samples (PMeT was deposited onto TO previously covered with PPy). Different values of Q were used for both the PPy and the PMeT layer depositions. The thickness data for samples with $Q_{PMeT} = 25$ mC cm^{-2} are not present because the second layer (PMeT) is discontinuous in some samples. Similar data for the PPy layer of TO/PMeT/PPy samples (inverted sequence of deposition of polymer layers) are presented in Table 3.

The analysis of Tables 1 and 2 permits us to observe that PMeT films deposited onto TO/PPy present thickness values larger than PMeT films deposited onto bare TO. Furthermore, the PMeT film thickness is independent of the thickness of the previously deposited PPy film. The roughness values, contrarily, are slightly reduced when compared to films grown on bare TO. It is important again to stress that the roughness R_a of the TO/PPy/PMeT films is constant for each Q_{PMeT} value, independent of the thickness of the previously deposited PPy film. This fact is interesting, since for TO/PPy films it was observed that $R_a\approx0.45d$ [12], indicating that the PMeT films grown onto TO/PPy are capable of producing a smoother surface than PPy onto bare TO. Owing to the low mobility of charge carriers in PPy [12] there is a significant potential drop along the film, perpendicular to the TO/polymer interface, during the deposition process. Our results suggest that PMeT preferentially deposits in PPy-film valleys, where the film thickness is lower and the potential more favorable, reducing the final roughness. It is not clear, however, why this behavior is not observed in homolayers. Speculatively, it is reasonable that phase segregation has an

Table 2 PMeT layer thickness (d_{PMeT}) of TO/PPy/PMeT samples for different Q_{PMeT} and Q_{PPy} combinations

	Q_{PMeT} (mC cm^{-2})			
	100	75	50	35
	d_{PMeT} (nm)			
Q_{PPy} (mC cm^{-2})				
100	–	461.7 ± 13.2	388.1 ± 10.5	120.5 ± 13.7
75	485.2 ± 85.2	445.1 ± 22.5	366.5 ± 67.6	100.7 ± 18.7
50	488.3 ± 50.0	468.7 ± 10.5	365.3 ± 51.2	110.1 ± 23.5
35	510.6 ± 21.7	472.1 ± 24.7	380.7 ± 47.2	118.4 ± 37.2
25	491.3 ± 25.7	467.2 ± 12.6	360.2 ± 21.3	101.2 ± 36.1

Table 3 PPy layer thickness (d_{PPy}) of TO/PMeT/PPy samples for different Q_{PPy} and Q_{PMeT} combinations

	Q_{PPy} (mC cm^{-2})			
	100	75	50	35
	d_{PPy} (nm)			
Q_{PMeT} (mC cm^{-2})				
100	–	320.3 ± 25.7	270.4 ± 42.9	182.4 ± 20.8
75	628.5 ± 67.9	305.6 ± 14.3	221.2 ± 23.7	152.7 ± 12.7
50	543.9 ± 24.5	261.2 ± 33.1	151.2 ± 54.6	115.7 ± 22.3
35	451.3 ± 60.7	243.5 ± 21.1	132.9 ± 50.1	92.4 ± 11.3
25	367.7 ± 32.7	200.6 ± 30.5	127.5 ± 61.2	67.8 ± 19.7

important contribution, making only those regions with highly favorable potential suitable for effective deposition of the second layer.

PPy films grown onto TO/PMeT behave quite differently. The PPy film thickness, apart from its dependence on Q_{PPy}, presents a strong dependence on the thickness of the previously deposited PMeT layer, as can be seen in Table 3. The R_a values of TO/PMeT/PPy films tend to grow with the increase of the deposition variables, Q_{PMeT} and Q_{PPy}. Also in this case, the roughness of the double layer structure, TO/PMeT/PPy, is lower than that of a single polymer layer, TO/PMeT ($R_a \approx 0.37d$) [11] or TO/PPy ($R_a \approx 0.45d$) [12].

The TO/PPy/PMeT samples are rougher than the TO/PMeT/PPy samples. This is confirmed by the micrographs presented in Figs. 1 and 2. It can be seen that TO/PPy/PMeT has a more porous surface morphology, with large globules (the same morphology of PPy onto TO [12]). This morphology predominates in the TO/PPy/PMeT film and possibly the PMeT film is able to penetrate into the PPy structure. These micrographs also confirm that the PPy morphology is strongly influenced by the substrate. The PPy films grown on TO/PMeT produce a smoother surface than the PPy films grown on TO [12].

Optical characteristics of PPy/PMeT and PMeT/PPy bilayers

The absorption spectra of PPy, PMeT, PPy/PMeT and PMeT/PPy bilayers are shown in Fig. 3. Also in this case, the bilayer absorption spectrum is the overlap of the two individual polymer spectra and its peaks are broader and less defined than the PMeT peak at ~500 nm. In the bilayer spectra the absorption edges are slightly shifted to longer wavelengths. This red shift is an indication that the polymers in the bilayers present, to

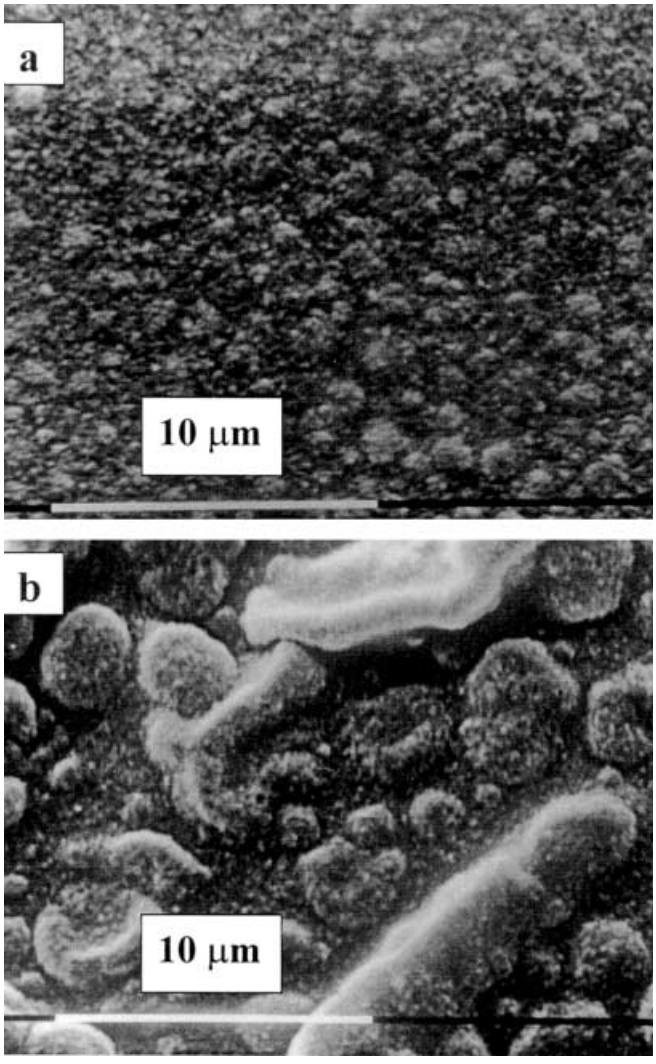

Fig. 1 SEM micrographs of TO/PPy/PMeT bilayers: **a** $Q = 25$ mC cm^{-2} for both layers; **b** $Q = 100$ mC cm^{-2} for both layers

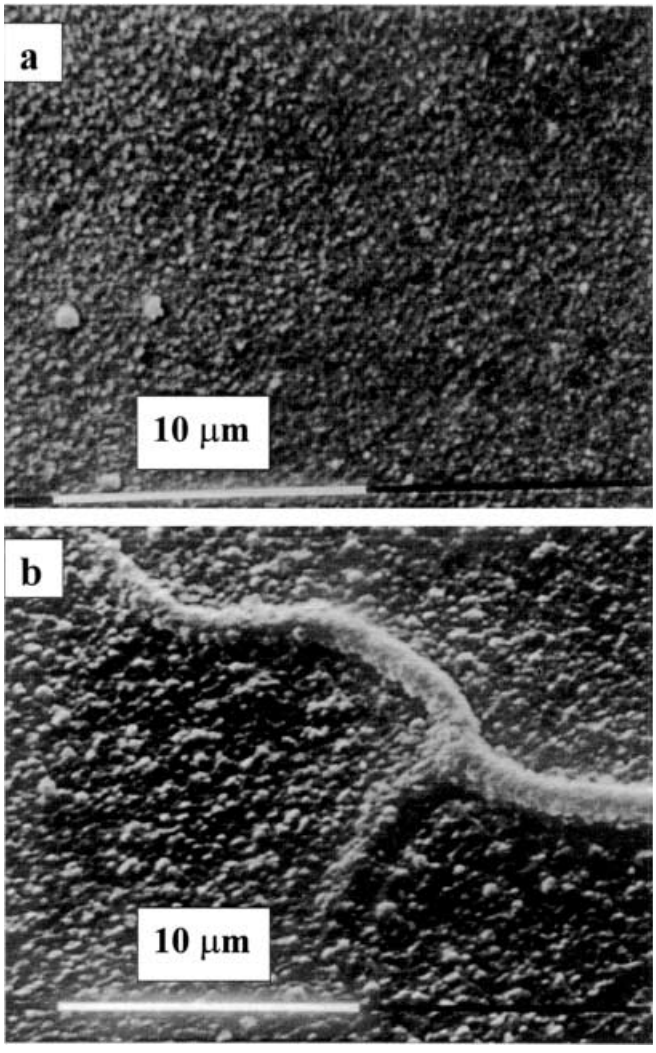

Fig. 2 SEM micrographs of TO/PMeT/PPy bilayers: **a** $Q = 25$ mC cm^{-2} for both layers; **b** $Q = 100$ mC cm^{-2} for both layers

some extent, a material fraction that has a lower energy gap than the individual polymers. This low-energy tail can be a consequence of energetic disorder that is expected to be increased in the PPy/PMeT and PMeT/PPy interfaces owing to a highly non-homogeneous local molecular environment.

Electrical characteristics of TO/PPy/PMeT/Al and TO/PMeT/PPy/Al samples

Al and TO are expected to have similar work function values, ~4.3 eV. This electrode material choice applies in the absence of a built-in electric field under zero bias, simplifying the analysis of the $I(V)$ data.

In Fig. 4 we present the $I(V)$ characteristics of a TO/PPy/PMeT/Al device. Qualitatively, this curve shape is typical for all TO/PPy/PMeT/Al devices. These $I(V)$ curves are highly asymmetrical, as exemplified by Fig. 4.

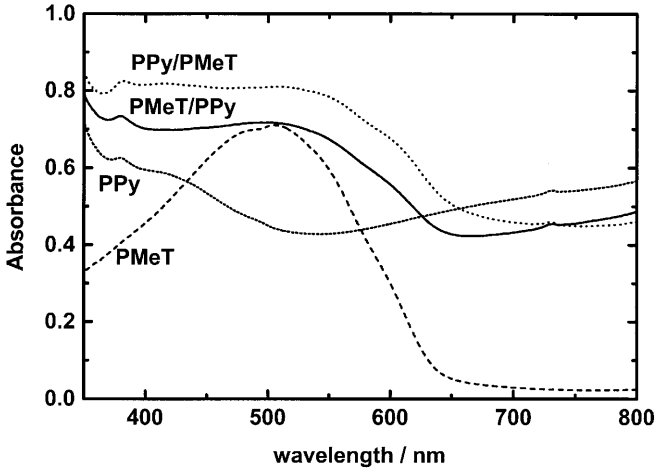

Fig. 3 Absorption spectra of PPy, PMeT, PMeT/PPy and PPy/PMeT. For all the films prepared, each film had $Q = 25$ mC cm^{-2}. $V = -0.5$ V versus Ag/AgCl

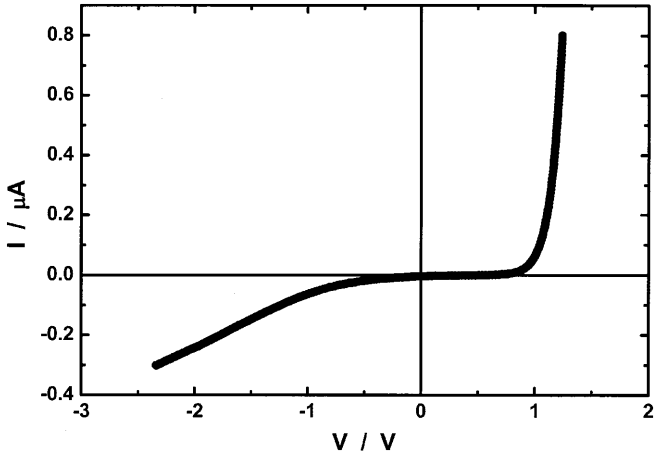

Fig. 4 $I(V)$ characteristics of a TO/PPy/PMeT/Al device. Preparation conditions: $Q_{PPy} = 75$ mC cm^{-2}; $Q_{PMeT} = 100$ mC cm^{-2}. $V \equiv V_{TO} - V_{Al}$

For TO positively biased, the slope of the linear log-log plot region $\partial \log I / \partial \log V \equiv \alpha$ lies in the range $6.9 < \alpha < 12.4$. The value of α depends on the thickness of both layers and varies from sample to sample, so that no clear correlation with layer thickness or interface roughness can be inferred. For TO negatively biased, $1.9 < \alpha < 2.1$ in the linear log-log region, strongly suggesting space-charge limited transport.

In the case of space-charge limited conduction, it is expected that:

$$j = \frac{9}{8} \mu_{eff} \varepsilon \frac{V^2}{d^3} \tag{2}$$

where j is the current density, μ_{eff} is the effective mobility and ϵ is the dielectric constant of the medium. It is intriguing that $\partial \log I / \partial \log d \approx -3$ at constant V for samples

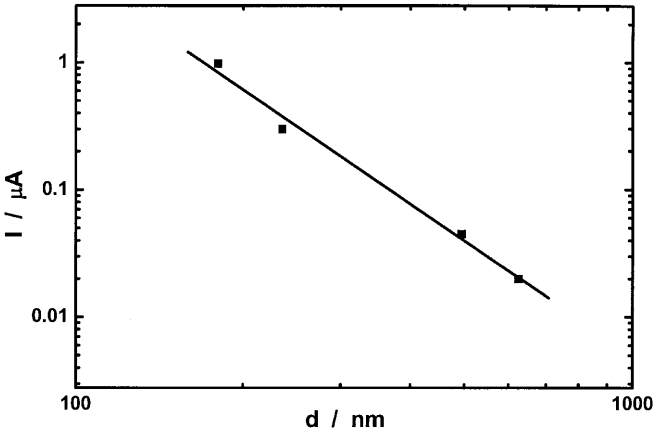

Fig. 5 $I(d_{total})$ dependence of different TO/PPy/PMeT/Al devices at constant $V = 0.8$ V. Preparation conditions: Q_{PMeT} = variable; $Q_{PPy} = 35$ mC cm^{-2}; $V \equiv V_{Al} - V_{TO}$

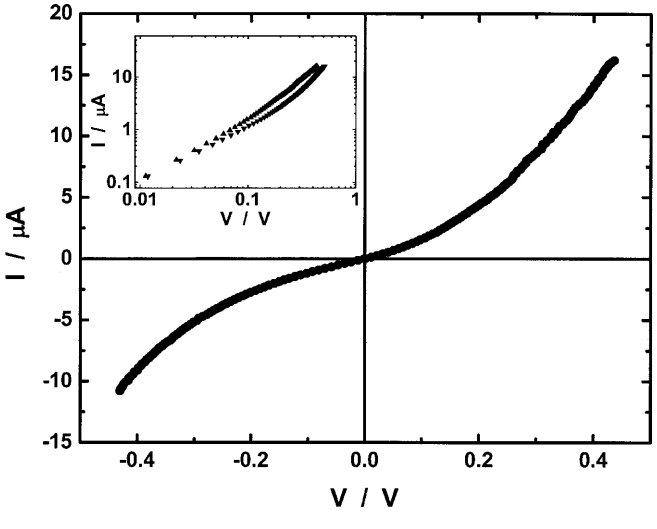

Fig. 6 $I(V)$ characteristics of a TO/PMeT/PPy/Al device. Preparation conditions: $Q_{PPy} = 35$ mC cm^{-2}; $Q_{PMeT} = 75$ mC cm^{-2}. $V \equiv V_{TO} - V_{Al}$. *Inset*: $I(V)$ characteristics of the same TO/PMeT/PPy/Al device in log-log form. *Down triangles*: $V \equiv V_{TO} - V_{Al} < 0$; *up triangles*: $V \equiv V_{TO} - V_{Al} > 0$

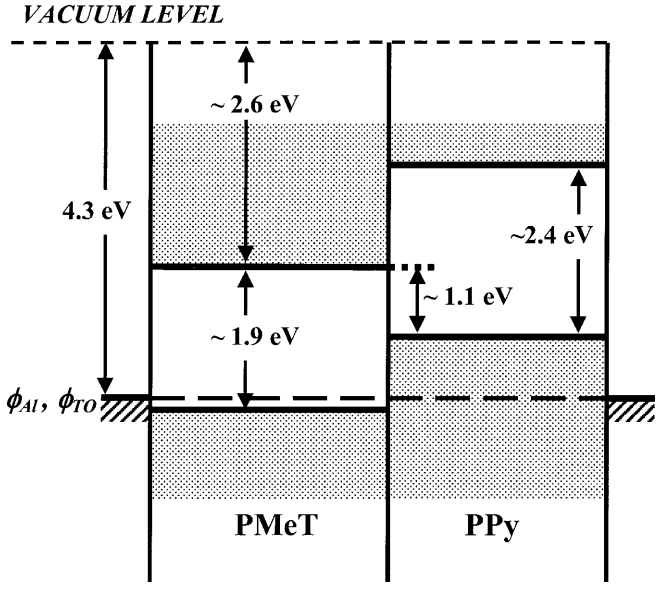

Fig. 7 Energy levels of the structures investigated in this work. For PMeT, the lowest unoccupied energy level is located at ~2.6 eV of the vacuum level and the energy gap is ~1.9 eV [11]. For PPy, these values are ~1.3 eV and 2.4 eV, respectively [12]

with different bilayer thickness (sum of the thickness of both layers). This is verified for the total bilayer thickness values of all columns or lines of Table 2 and is exemplified in Fig. 5. Assuming $\epsilon_{PPy} = \epsilon_{PMeT} \approx 3$ and fitting Eq. 2 to the experimental data range where $j \propto V^2$, $\mu_{eff} = (3.0 \pm 1.0) \times 10^{-10}$ cm^2 V^{-1} s^{-1} was determined.

In Fig. 6 we present the $I(V)$ characteristics of a TO/PMeT/PPy/Al device. Qualitatively, this curve shape is typical for all TO/PMeT/PPy/Al devices. As can be seen in Fig. 6, these $I(V)$ curves present asymmetry. In spite of the asymmetry, at both polarities, $V \equiv V_{TO} - V_{Al} < 0$ and $V \equiv V_{TO} - V_{Al} > 0$, there are segments of the $I(V)$ curve that follow $j \propto V^2$, as exemplified in the inset. This behavior is observed for samples with the deposition parameter combinations of Table 3, with only three exceptions, namely ($Q_{PMeT} = 100$ mC cm^{-2}; $Q_{PPy} = 100$ mC cm^{-2}), ($Q_{PMeT} = 100$ mC cm^{-2}; $Q_{PPy} = 75$ mC cm^{-2}) and ($Q_{PMeT} = 100$ mC cm^{-2}; $Q_{PPy} = 50$ mC cm^{-2}). Also in this case, taking the segments where $j \propto V^2$, it was observed that $\partial \log I / \partial \log d \approx -3$ at constant V for samples with different bilayer thickness (sum of the thickness of both layers). Again, assuming $\epsilon_{PPy} = \epsilon_{PMeT} \approx 3$ and fitting Eq. 2 to the experimental data range where $j \propto V^2$, we determined $\mu_{eff} = (3.0 \pm 0.8) \times 10^{-10}$ cm^2 V^{-1} s^{-1} for $V \equiv V_{TO} - V_{Al} < 0$ and $\mu_{eff} = (1.3 \pm 0.6) \times 10^{-10}$ cm^2 V^{-1} s^{-1} for $V \equiv V_{TO} - V_{Al} > 0$.

An analysis of the data presented above is difficult, but it is evident that the bilayer structures behave electrically as a homolayer, whose effective mobility is of the order of 10^{-10} cm^2 V^{-1} s^{-1}. In previous work, the effective mobility of positive charge carriers in PMeT [11] and PPy [12] was determined, being 4×10^{-4} cm^2 V^{-1} s^{-1} and 8×10^{-10} cm^2 V^{-1} s^{-1}, respectively. The effective bilayer mobility of the positive charge carriers is quite near to their mobility in PPy. Only TO/PPy/PMeT/Al devices, with TO positively biased on the internal interface (see Fig. 7), seem to play an important role in the transport limitation. $I(V)$ curves of TO/PMeT/PPy/Al devices with TO positively biased do not present this effect. Apparently, the higher roughness of TO/PMeT produces a less defined PMeT/PPy interface that under bias and space-charge accumulation conditions does not operate as an effective barrier for charge injection. For this reason, PPy/PMeT interfaces are expected to be more effective in exciton dissociation than PMeT/PPy interfaces.

Conclusion

We have reported the successive deposition of polypyrrole and poly(3-methylthiophene) layers by an electrochemical method onto a tin oxide-covered glass substrate. We have shown that polymer bilayer thickness and roughness depend on the deposition conditions as well as on the sequence of deposition of the polymeric layers. The charge transport characteristics of these bilayer devices were investigated and an effective charge carrier mobility of the order of 10^{-10} cm^2 V^{-1} s^{-1} was determined. In spite of the energy level discontinuity expected at the polymer/polymer interface, clear evidence of charge transport limitation due to this interface was observed only in case of TO/PPy/PMeT/Al devices biased so that $V_{TO} > V_{Al}$, i.e. TO injecting positive charge carriers.

Acknowledgements The authors would like to thank PADCT/CNPq (project 62.81/97-0 CEMAT) for financial support. I.A.H. acknowledges CNPq for a research fellowship. R.V. acknowledges CAPES for a scholarship. The authors also thank the "Centro de Microscopia Eletrônica-UFPR" for SEM facilities.

References

1. Friend RH, Greenham NC (1998) Electroluminescence in conjugated polymers. In: Skotheim TA, Elsenbaumer RL, Reynolds JR (eds) Handbook of conducting polymers. Dekker, New York, p 823
2. Khramtchenkov DV, Bässler H, Arkhipov VI (1996) J Appl Phys 79:9283
3. Berleb S, Brütting W, Paasch G (2000) Org Electron 1:41
4. Krone BK, Davis PS, Campbell IH, Smith DL (21) J Appl Phys 87:1974
5. Shaheen SE, Brabec CJ, Sariciftci NS, Padinger F, Fromherz T, Hummelen JC (2001) Appl Phys Lett 78:841
6. Gazotti WA, Nogueira AF, Girotto EM, Micaroni L, Martini M, das Neves S, De Paoli MA (2001) Optical devices based on conductive polymers. In: Nalwa HS (ed) Handbook of advanced electronic and photonic materials and devices, vol 10. Academic Press, New York, pp 53
7. Aizawa M, Yamada T, Shinohara H, Akagi K, Shirakawa H (1986) J Chem Soc Chem Commun 1315
8. Kaneto K, Takeda S, Yoshino K (1985) Jpn J Appl Phys 24:L553
9. Usuki A, Murase M, Kurauchi T (1987) Synth Met 18:705
10. Onoda M, Tada K, Zakhidov AA, Yoshino K (1998) Thin Solid Films 331:76

11. Valaski R, Bozza AF, Micaroni L, Hümmelgen IA (2000) J Solid State Electrochem 4:390
12. Valaski R, Ayoub S, Micaroni L, Hümmelgen IA (2001) Thin Solid Films 338:171
13. Yadava YP, Denicoló G, Arias AC, Roman LS, Hümmelgen IA (1997) Mater Chem Phys 48:263
14. Whitehouse DT (1994) Handbook of surface metrology. Institute of Physics, Bristol, p 14
15. Arias AC, Roman LS, Kugler T, Toniolo R, Meruvia MS, Hümmelgen IA (2000) Thin Solid Films 371:201
16. Lide DR (1995) CRC handbook of chemistry and physics. CRC Press, Boca Raton, pp
17. Roman LS, Denicoló I, Nart FC, Hümmelgen IA (1996) J Mater Sci Lett 15:1307